Application of LMS-Based NN Structure for Power Quality Enhancement in a Distribution Network Under Abnormal Conditions

Rahul Kumar Agarwal, Ikhlaq Hussain, *Member, IEEE*, and Bhim Singh, *Fellow, IEEE*

***Abstract*— This paper proposes an application of a least mean-square (LMS)-based neural network (NN) structure for the power quality improvement of a three-phase power distribution network under abnormal conditions. It uses a single-layer neuron structure for the control in a distribution static compensator (DSTATCOM) to attenuate the harmonics such as noise, bias, notches, dc offset, and distortion, injected in the grid current due to connection of several nonlinear loads. This admittance LMS-based NN structure has a simple architecture which reduces the computational complexity and burden which makes it easy to implement. A DSTATCOM is a custom power device which performs various functionalities such as harmonics attenuation, reactive power compensation, load balancing, zero voltage regulation, and power factor correction. Other main contribution of this paper involves operation of the system under abnormal conditions of distribution network which means noise and distortion in voltage and imbalance in three-phase voltages at the point of interconnection. For substantiating and demonstrating the performance of proposed control approach, simulations are carried on MATLAB/Simulink software and corresponding experimental tests are conducted on a developed prototype in the laboratory.**

***Index Terms*— Distribution network, distribution static compensator (DSTATCOM), least mean-square (LMS), neural network (NN), power quality.**

I. Introduction

WITH the ever increasing electric power demand, it is evident for the power distribution networks to be constantly stressed out and laden with various abnormalities and fault conditions. Over the years, compensation devices like custom power devices (CPDs) have proved effective in alleviating such abnormalities present in the distribution networks. Where the response time of the protection and compensation devices is one major area of concern which is continuously being focused upon and its related technologies are persistently being improved. Neural networks (NNs) have revolutionized this area by reducing the computational complexity and burden associated with the control algorithms of the CPDs in order to make them and perform faster with increased ability in response and fault clearing times as well as better stability of the system [1]. Today, due to its parallelized computations and generic nature, NN is applied to almost every control structure. Xie *et al*. [2] have proposed an application of adaptive dynamic programming-based NN in vehicle-to-grid networks to control the scheduling of electrical loads of electric vehicles. Mishra [3] has proposed a H∞-learning method for updating of NN-based radial basis function employed for a unified power flow controller. Another application of NN is proposed in the literature [4] which introduces the learning framework and dynamic adaptive programming for energy management system in smart micro-grid.

Nonlinear loads connected at the point of interconnection (PoI) of the distribution network have consistently degrading supply power quality by injecting harmonics in the supply current. Among the available CPDs for power quality improvement, distribution static compensator (DSTATCOM) is the most versatile one [5]. It is a solid-state controller derived from power electronics which is used to perform power conditioning of a distribution network [6]. Apart from attenuating harmonics, DSTATCOM performs functions like power factor correction, zero voltage regulation, supply currents balancing, etc. Several control algorithms have been proposed in the literature for the functioning of a DSTATCOM [7]. Kumar *et al.* [8] have proposed a dual voltage source inverter as a CPD for efficient power conditioning where an analysis has been done for unbalanced and nonlinear loaded conditions. The system has more losses due to increased number of devices, and it does not show performance under abnormal conditions of distribution network. An interactive DSTATCOM system has been proposed in [9] which can operate under voltage control mode as well as current control mode and transition from one state to another without disturbing the network performance. Srinivas *et al*. [10] have proposed a combined least mean-square (LMS)/least mean-fourth-based control algorithm for DSTATCOM showing the response of the internal signals under varying loading conditions. Some other DSTATCOM control algorithms include variable forgetting factor recursive least-square-based control [11], hybrid voltage control [12], adaptive noise cancellation-based control [13], and anti-windup-based control approach [14]. Wherein these publications lack to show performance of the system under abnormal conditions which is the most usual

Manuscript received May 18, 2016; revised December 05, 2016 and February 17, 2017; accepted February 20, 2017. Date of publication March 16, 2017; date of current version April 16, 2018. This work was supported by the Department of Science and Technology, Government of India under Grant RP02583.

The authors are with the Department of Electrical Engineering, Indian Institute of Technology Delhi, New Delhi-110016, India (e-mail: rahul.agarwal990@gmail.com; ikhlaqiitd@gmail.com; bsingh@ee.iitd.ac.in).

Color versions of one or more of the figures in this paper are available online at http://ieeexplore.ieee.org.

Digital Object Identifier 10.1109/TNNLS.2017.2677961

cases with the distribution networks like system operating under distorted and imbalanced three-phase voltages at the PoI.

LMS has been first proposed in [15]. From that time, continuous evolutions have taken place and numerous applications have been put forward. Here, LMS-based NN structure is utilized for attenuating the effects of harmonics injected in the supply current by the nonlinear loads. Harmonics are treated as errors in the supply current; therefore, LMS is used to extract fundamental component of the load current and to minimize the error which is an iterative process. At each iteration, respective filtered weights are updated. Here, admittance of the load is first calculated and then weights of the admittance is filtered and updated. Of the several benefits of LMS algorithm, simple, ease of implementation, generalized nature, parallel processing, high digital signal processing (DSP) speed, reduced computational burden, reduced response time, and high sampling rate are some of the benefits which make it outstanding for applications such as it. Carvajal *et al.* [16] have discussed an analysis on the effects of interaction between soft-computing LMS algorithm and hardware devices for real-time implementation. A mean-square convergence analysis has been carried out in the literature [17] as well as some misconceptions related to LMS learning algorithm and revised response of convergence have been presented in [18]. Moreover, convergence performances of LMS and normalized LMS have been analyzed in [19] which show that normalized LMS performs better than LMS. The system, which is proposed here, has the inputs selected for LMS algorithm which are already in the normalized state so the performance of convergence is better. The convergence relates to how fast and how much the errors are minimized in the system.

This paper proposes an admittance LMS-based NN control algorithm for a DSTATCOM for enhancing the power quality of a three-phase distribution network subjected to nonlinear and unbalanced loading under distorted and imbalanced three-phase voltages at the PoI. There are international standards for validating the performance of the system such as the IEEE-519 standard for harmonics [20] and the IEEE-1453 for voltage flickers and fluctuations [21]. Therefore, for demonstrating the effectiveness of the system, simulations are carried out in MATLAB Simulink and tests are conducted on the established prototype in the laboratory. The obtained results are recorded and analyzed in light of the IEEE standards.

II. System Configuration

The schematic of proposed system topology is shown in Fig. 1. The circuitry of system has three main components, which are three-phase distribution grid, loads, and DSTATCOM. The proposed work includes the use of a three-leg voltage source converter (VSC) which acts as a DSTATCOM to produce compensating currents. Interfacing inductors are used to connect the VSC with the three-phase distribution grid. Moreover, to reduce the ripples present in the PoI voltages, a ripple filter is connected. The comprehensive experimental and design data are specified in the Appendix.

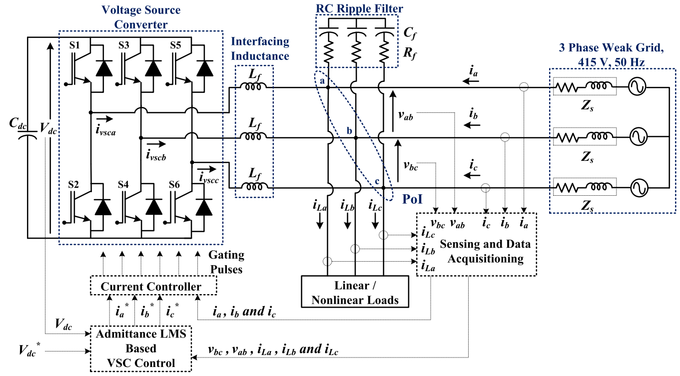

Fig. 1. Proposed system topology.

III. Control Algorithm

The control architecture of the system is shown in Fig. 2(a). The control algorithm is derived using the admittance LMS-based NN technique for effective switching of the VSC.

A. Estimation of Unit Templates

From the sensed PoI voltages (v_{ab} and v_{bc}), the phase voltages (v_a, v_b, v_c) are obtained from equations in [22] as

$$v_a = \frac{2v_{ab} + v_{bc}}{3}; \quad v_b = \frac{-v_{ab} + v_{bc}}{3}; \quad v_c = \frac{-v_{ab} - 2v_{bc}}{3}. \tag{1}$$

To reduce the influence of imbalances and distortion of the grid voltages on the responses of system, a filtering method is utilized. These v_a, v_b, and v_c are fed through a bandpass filter having cutoff frequencies (upper limit $\omega_u = 2\pi{*}52$ rad/s and lower limit $\omega_l = 2\pi{*}48$ rad/s) to eliminate the harmonics distortion in grid voltages. To decrease the effect of grid voltages imbalances, the positive sequence (v_{pa}, v_{pb}, and v_{pc}) of the grid voltages is estimated as

$$\begin{pmatrix} v_{pa} \\ v_{pb} \\ v_{pc} \end{pmatrix} = \frac{1}{3}\begin{pmatrix} 1 & a^2 & a \\ a & 1 & a^2 \\ a^2 & a & 1 \end{pmatrix} \times \begin{pmatrix} v_a \\ v_b \\ v_c \end{pmatrix} \tag{2}$$

where $a = 1\angle 120^\circ$ and $a^2 = 1\angle 240^\circ$.

After evaluating v_{pa}, v_{pb}, and v_{pc} the peak of Point of common coupling voltage, in-phase and quadrature components are evaluated as

$$V_t = \sqrt{\frac{2}{3}\left(v_{pa}^2 + v_{pb}^2 + v_{pc}^2\right)}$$
$$u_{pa} = \frac{v_{pa}}{V_t}; \quad u_{pb} = \frac{v_{pb}}{V_t}; \quad u_{pc} = \frac{v_{pc}}{V_t} \tag{3}$$

$$u_{qa} = -\frac{u_{pb}}{\sqrt{3}} + \frac{u_{pc}}{\sqrt{3}}; \quad u_{qb} = \frac{\sqrt{3}u_{pa}}{2} + \frac{(u_{pb} - u_{pc})}{2\sqrt{3}}$$
$$u_{qc} = -\frac{\sqrt{3}u_{pa}}{2} + \frac{(u_{pb} - u_{pc})}{2\sqrt{3}}. \tag{4}$$

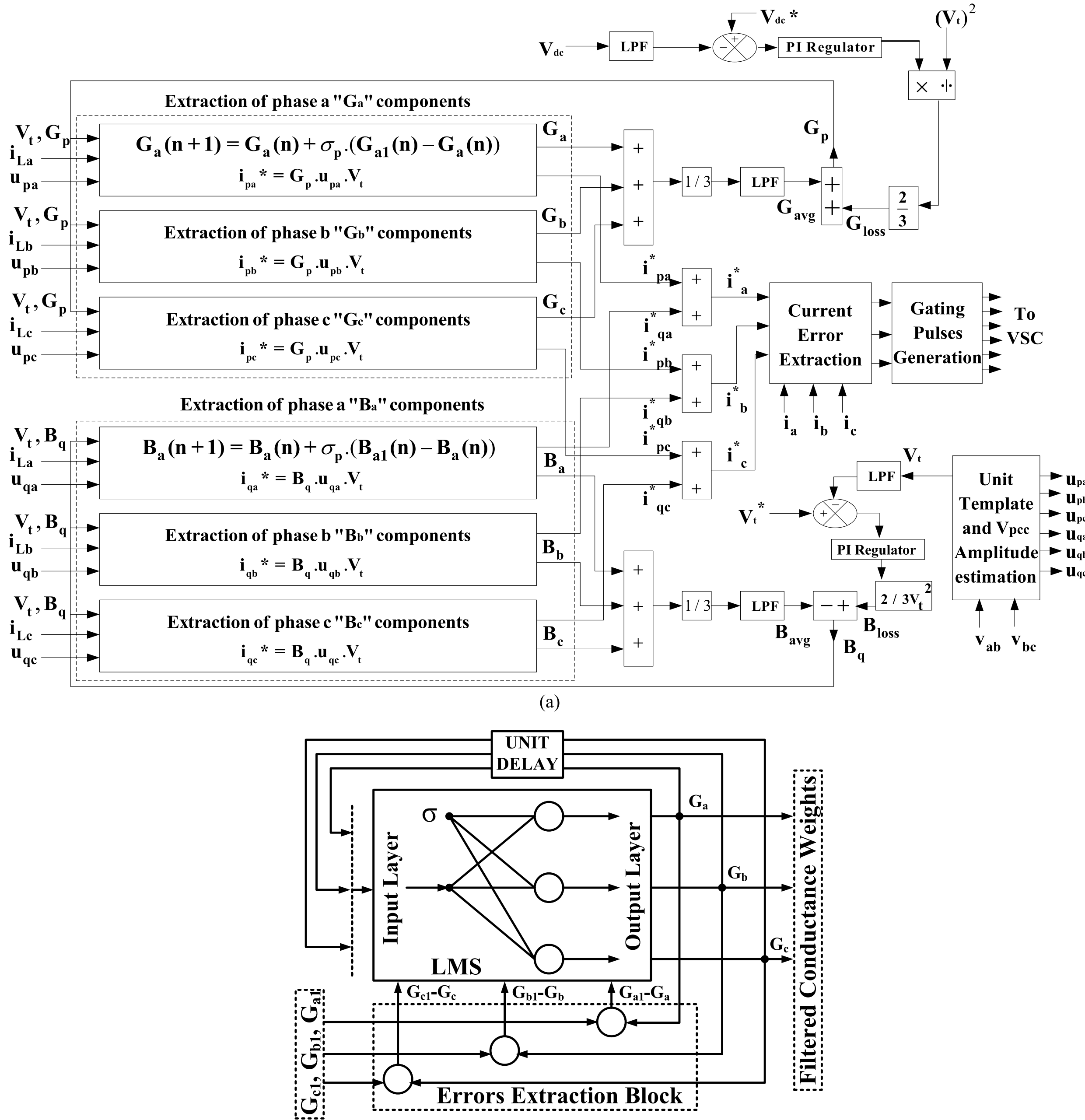

(a)

(b)

Fig. 2. (a) Control structure of admittance LMS technique. (b) Block diagram of admittance LMS-based NN.

B. Estimation of Admittances of Loss Components

After the evaluation of V_t, the voltage error $V_{\mathrm{te}}(n)$ of the voltage at the PoI and the reactive loss component (Q_{loss}) is estimated as

$$V_{\mathrm{te}}(n) = V_t^*(n) - V_t(n) \quad (5)$$

$$Q_{\mathrm{loss}}(n+1) = Q_{\mathrm{loss}}(n) + K_{\mathrm{pt}}\{V_{\mathrm{te}}(n+1) - V_{\mathrm{te}}(n)\} + K_{\mathrm{it}}V_{\mathrm{te}}(n+1). \quad (6)$$

Therefore, the susceptance loss component is estimated as

$$B_{\mathrm{loss}}(n) = \frac{2Q_{\mathrm{loss}}(n)}{3V_t^2} \quad (7)$$

where K_{it} and K_{pt} are the integral gain and proportional gain constants utilized in proportional integral (PI) ac voltage controller.

Likewise, the dc-link voltage error (V_{de}) and the active loss component (P_{loss}) are calculated as

$$V_{\mathrm{de}}(n) = V_{\mathrm{dc}}^*(n) - V_{\mathrm{dc}}(n) \quad (8)$$

$$w_{\mathrm{cp}}(n+1) = w_{\mathrm{cp}}(n) + K_{\mathrm{pd}}\{V_{\mathrm{de}}(n+1) - V_{\mathrm{de}}(n)\} + K_{\mathrm{id}}V_{\mathrm{de}}(n+1). \quad (9)$$

Therefore, the conductance loss component is estimated as

$$G_{\mathrm{loss}}(n) = \frac{2P_{\mathrm{loss}}(n)}{3V_t^2} \quad (10)$$

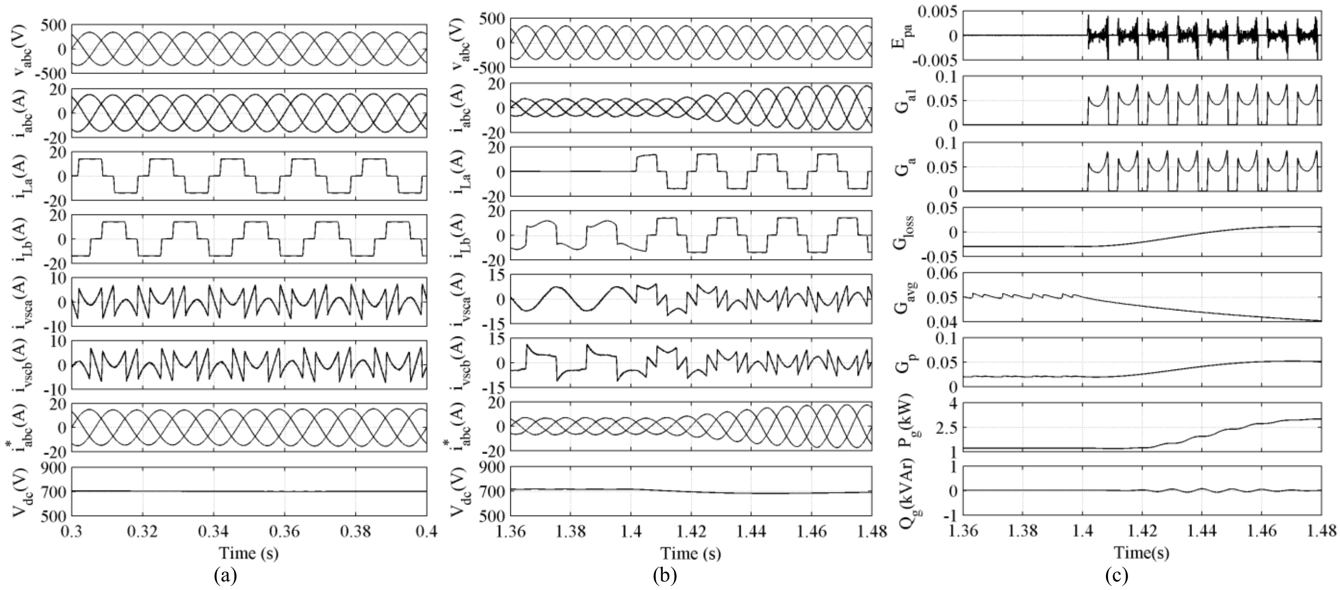

Fig. 3. (a) Steady-state performance subjected to nonlinear load. (b) Dynamic response subjected to unbalanced nonlinear load. (c) Response of internal signals under unbalanced nonlinear load.

where $K_{\rm id}$ and $K_{\rm pd}$ are the integral gain and proportional gain constants utilized in PI dc-link voltage controller.

The total admittance value of loss component is estimated as

$$Y_{\rm loss}(n) = G_{\rm loss}(n) + j \cdot B_{\rm loss}(n). \tag{11}$$

C. Extraction of Filtered Admittance Components Using LMS-Based NN Structure

Fig. 2(b) shows the block diagram of admittance LMS-based NN structure. The conductance of fundamental in-phase component of phase "a" of load current is estimated as

$$G_a(n+1) = G_a(n) + \sigma \cdot \{G_{a1}(n) - G_a(n)\} \tag{12}$$

$$G_{a1}(n) = \frac{u_{\rm pa}(n) \cdot i_{La}(n).V_t}{v_{\rm pa}^2} \tag{13}$$

where $v_{\rm pa}$, $i_{\rm La}(n)$, σ, and $u_{\rm pa}(n)$ are the voltage, load current, adaptation rate, and in-phase unit template at the nth instant of phase "a," respectively.

Similarly, the conductance of the fundamental in-phase load current components of phases "b" and "c" is estimated as

$$G_b(n+1) = G_b(n) + \sigma \cdot \{G_{b1}(n) - G_b(n)\} \tag{14}$$

$$G_c(n+1) = G_c(n) + \sigma \cdot \{G_{c1}(n) - G_c(n)\}. \tag{15}$$

The susceptance of quadrature fundamental component of phase "a" of the load current is estimated as

$$B_a(n+1) = B_a(n) + \sigma \cdot \{B_{a1}(n) - B_a(n)\} \tag{16}$$

$$B_{a1}(n) = \frac{u_{\rm qa}(n) \cdot i_{\rm La}(n) \cdot V_t}{v_{\rm pa}^2} \tag{17}$$

where $u_{\rm qa}(n)$ and $i_{\rm La}(n)$ are the quadrature unit template and the load current at the nth instant of phase "a."

TABLE I

MAGNITUDES UNDER NONLINEAR LOAD

Mode	Parameters	Magnitude and THD
UPF	Grid current (A)	15.47 A, 1.33 %
	Load current (A	15.39 A, 28.34 %
	Grid voltage (V)	338.8 V, 0.14 %
	DC link Voltage (V)	700 V

Similarly, the susceptance of the quadrature fundamental load current components of phases "b" and "c" is estimated as

$$B_b(n+1) = B_b(n) + \sigma \cdot \{B_{b1}(n) - B_b(n)\} \tag{18}$$

$$B_c(n+1) = B_c(n) + \sigma \cdot \{B_{c1}(n) - B_c(n)\}. \tag{19}$$

D. Generation of Reference Grid Currents

The total active weight component is calculated as

$$G_p = G_{\rm avg} + G_{\rm loss} \tag{20}$$

where

$$G_{\rm avg} = (G_a + G_b + G_c)/3. \tag{21}$$

Now, the reference active components of grid currents ($i_{\rm pa}^*$, $i_{\rm pb}^*$, $i_{\rm pc}^*$) are expressed as

$$i_{\rm pa}^* = V_t \cdot G_p \cdot u_{\rm pa}; \quad i_{\rm pb}^* = V_t \cdot G_p \cdot u_{\rm pb}; \quad i_{\rm pc}^* = V_t \cdot G_p \cdot u_{\rm pc}. \tag{22}$$

Likewise, the total reactive weight component is evaluated as

$$B_q = B_{\rm loss} - B_{\rm avg} \tag{23}$$

where

$$B_{\rm avg} = (B_a + B_b + B_c)/3. \tag{24}$$

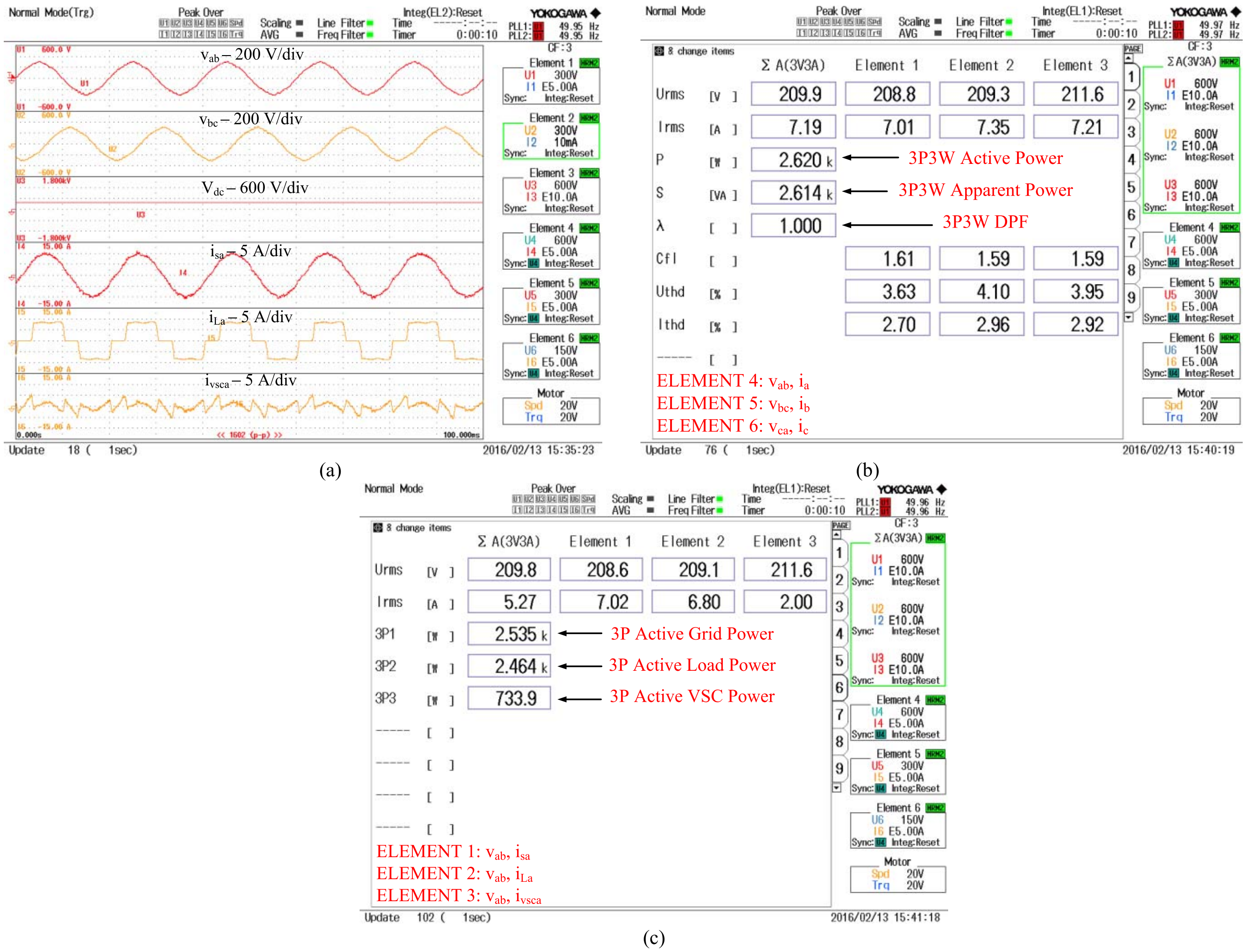

Fig. 4. Steady-state responses subjected to nonlinear load. (a) Waveforms of $v_{\rm ab}$, $v_{\rm bc}$, $V_{\rm dc}$, i_a, $i_{\rm La}$, and $i_{\rm vsca}$. (b) Magnitudes of the grid side parameters. (c) Magnitudes of the grid, load, and VSC side parameters.

Now, the reactive reference grid current components ($i^*_{\rm qa}$, $i^*_{\rm qb}$, $i^*_{\rm qc}$) are evaluated as

$$i^*_{\rm qa} = V_t \cdot B_p \cdot u_{\rm qa}; \quad i^*_{\rm qb} = V_t \cdot B_p \cdot u_{\rm qb}; \quad i^*_{\rm qc} = V_t \cdot B_p \cdot u_{\rm qc}. \tag{25}$$

So, the total reference grid currents (i^*_a, i^*_b, and i^*_c) are evaluated as

$$\begin{aligned} i^*_a &= i^*_{\rm pa} + i^*_{\rm qa} \\ i^*_b &= i^*_{\rm pb} + i^*_{\rm qb} \\ i^*_c &= i^*_{\rm pc} + i^*_{\rm qc}. \end{aligned} \tag{26}$$

E. Generation of Gating Signals Using Hysteresis Controller

For generation of the gating pulses, an indirect current control approach over reference grid currents and sensed grid currents is utilized here [7].

IV. Simulation Results

The model of proposed system is developed in MATLAB Simulink to demonstrate its performance. The essential components such as interfacing inductances, dc-link capacitor, and ripple filter, are designed and modeled as in [7] and [23]. The system is subjected to unbalanced and balanced load conditions (nonlinear loads) to verify the system performance. The design data of the system are given in the Appendix.

A. Performance Under Nonlinear Loads

Fig. 3(a) shows steady-state response of the system when subjected to a nonlinear load. From Fig. 3, it is understood that the grid currents ($i_{\rm abc}$) are free from harmonics and maintained sinusoidal owing to nonlinearity observed in load currents ($i_{\rm La}$ and $i_{\rm Lb}$). The waveforms of compensating currents ($i_{\rm vsca}$ and $i_{\rm vscb}$) are provided by VSC for unity power factor (UPF) operation of system. The dc-link voltage ($V_{\rm dc}$) is maintained at its constant value. Table I shows the magnitudes of total harmonics distortion (THD) in grid current, load current, and PoI voltage. The THD of load current is 28.34%, whereas the THD of the grid current is reduced to 1.33% which satisfies an IEEE-519 standard [20].

B. Performance Under Unbalanced Loads

For further analysis, the system is subjected to an unbalanced nonlinear load. The load from phase "*a*" is disconnected

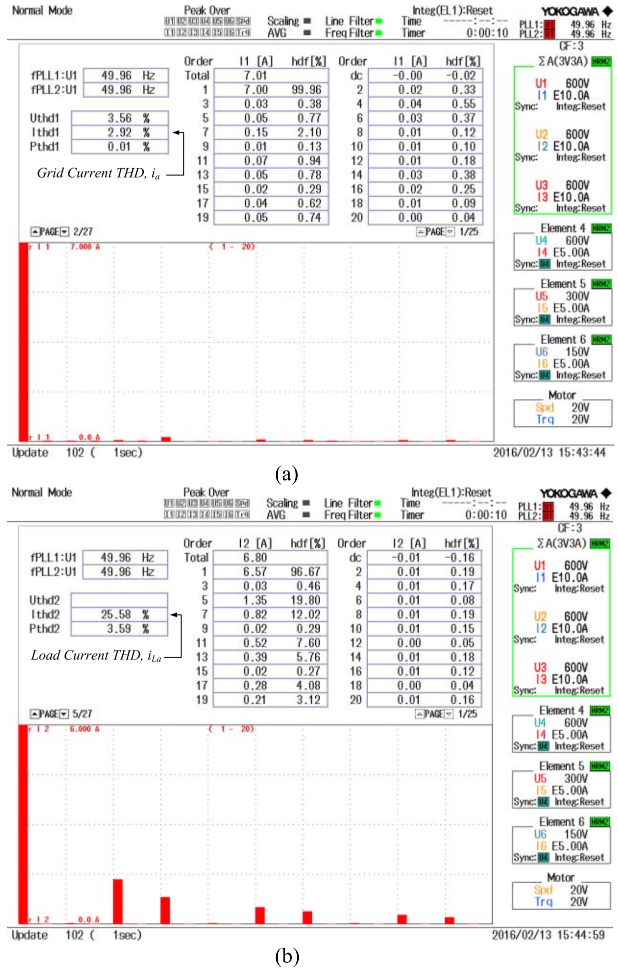

Fig. 5. (a) Harmonic spectrum and THD of grid current i_a. (b) Harmonic spectrum and THD of load current i_{La}.

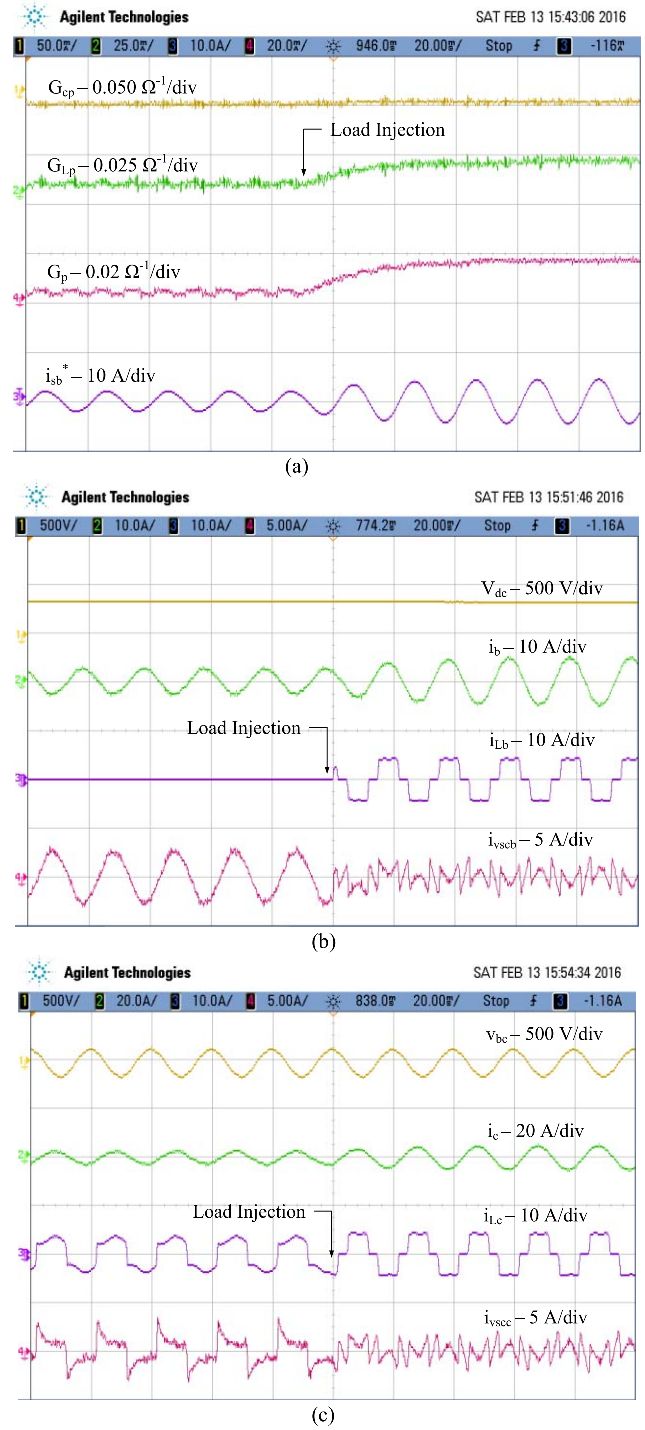

Fig. 6. (a) Response of internal signals of the proposed control algorithm under unbalanced load. (b) and (c) Dynamic responses under unbalanced nonlinear load.

from 1.36 to 1.4 s, and the dynamic response of the system is shown in Fig. 3(b) and (c). Fig. 3(b) shows the waveforms of grid currents (i_{abc}), load currents (i_{La} and i_{Lb}), and VSC currents (i_{vsca} and i_{vscb}) where grid currents are maintained sinusoidal as well as increased in magnitude as the load of phase "a" is injected back again. Fig. 3(c) shows the response of internal signals when the load is unbalanced. The variations are shown in the waveforms of error (E_{pa}), conductance values (G_{a1}, G_a, G_{loss}, G_{avg}, and G_{p}) and active and reactive powers (P_{g} and Q_{g}) supplied by the grid. The value of "E_{pa}" is zero until the load of phase "a" is injected back again. The active power (P_g) supplied by the grid is increased as the load is injected back as well as reactive power (Q_g) is nearly zero, i.e., the system operates at UPF mode.

V. Experimental Results

The prototype of the proposed system is developed in the laboratory which consists of VSC, inductors, RC filter, grid, nonlinear loads, DSP controller, optocouplers, voltage and current sensors, and measuring instruments. Hall-Effect current (LA55-P) and voltage (LV25-P) sensors are utilized to sense currents and voltages in the system, respectively. The proposed NN-based adaptive control is built on to DSP controller (DSPACE-Microlab Box-1202) using MATLAB. A power analyzer (YOKOGAWA make, WT-1800) and a DSO (Agilent make, DSO7014A) are used to measure and record the parameters and waveforms. The designed system data are given in the Appendix.

A. Performance Under Nonlinear Loads

Fig. 4(a)–(c) depicts the steady-state response of proposed DSTATCOM system subjected to nonlinear load.

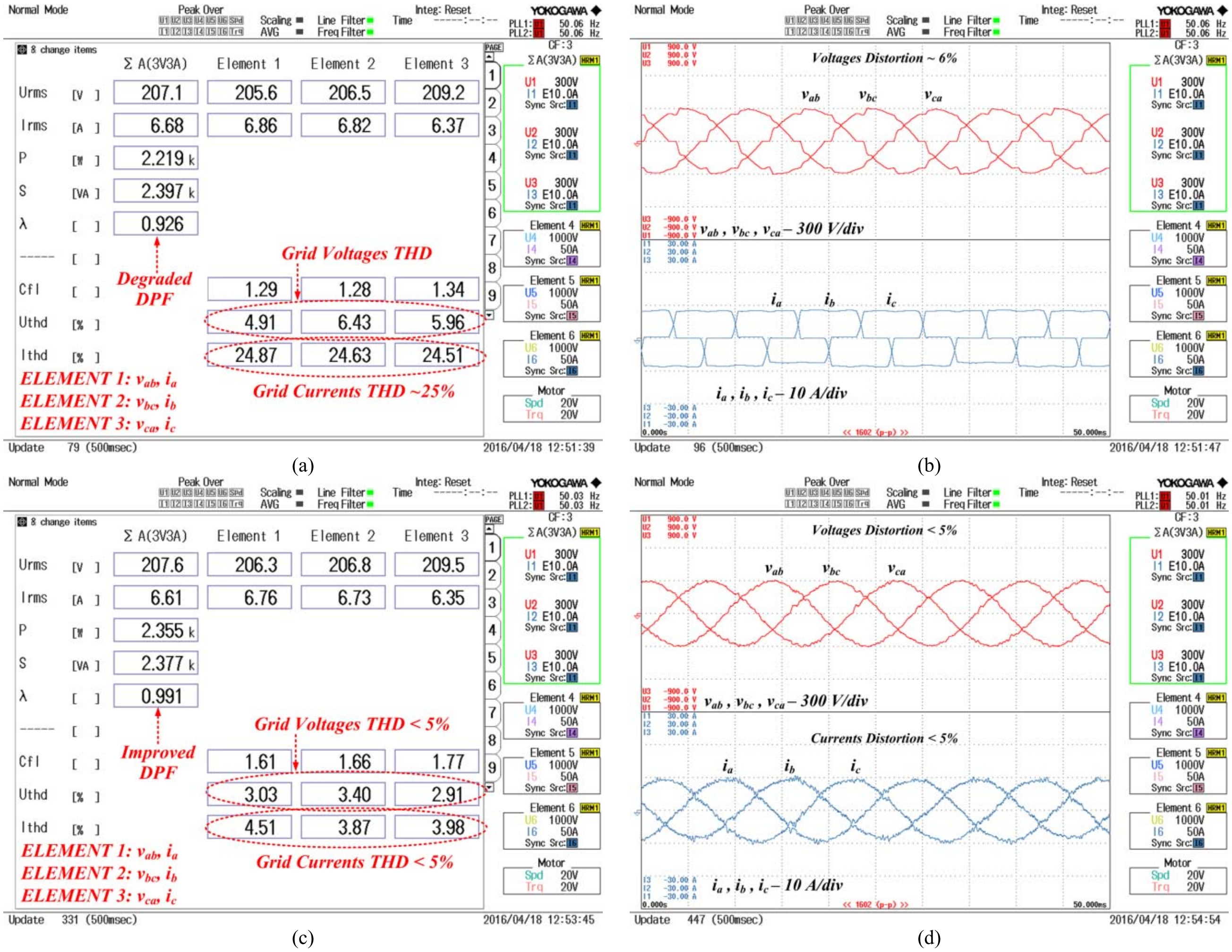

Fig. 7. (a) and (b) Performance under distorted grid voltages without DSTATCOM. (c) and (d) Performance under distorted grid voltages with DSTATCOM.

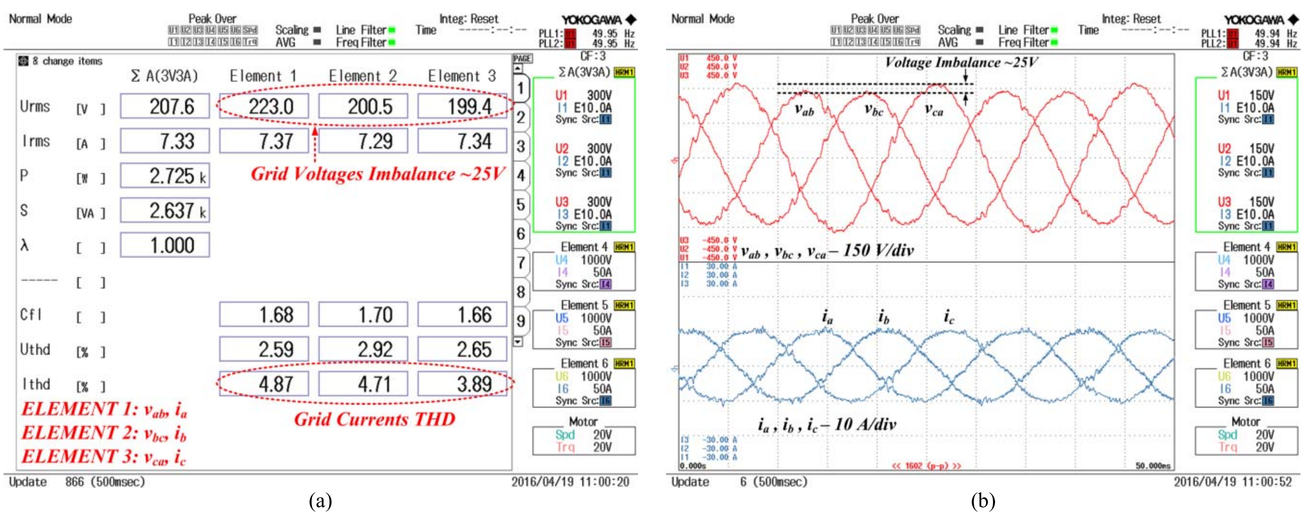

Fig. 8. (a) and (b) Performanceof the system under grid voltages imbalance condition.

In this Fig. 4(a), waveforms of v_{ab}, v_{bc}, v_{dc}, i_a, i_{La}, and i_{Ca} are shown. It is understood that the grid current (i_a) is free from harmonics and maintained sinusoidal owing to nonlinearity observed in the load current (i_{La}) which is compensated by DSTATCOM as shown i_{vsca}, while dc-link voltage is regulated at set value. Fig. 4(b) depicts the parameters of grid voltages (v_{ab}, v_{bc}, and v_{ca}) and grid currents (i_a, i_b, and i_c), active power (P) and apparent power (S), crest factor of grid currents,

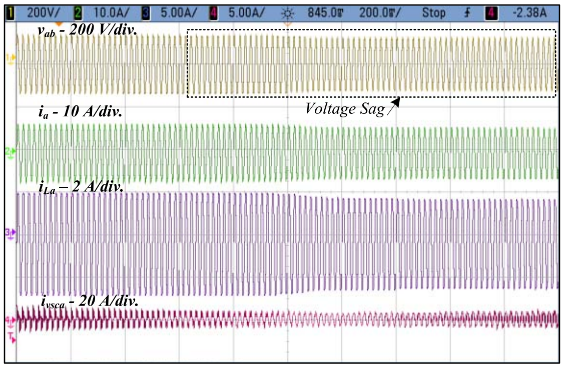

(a)

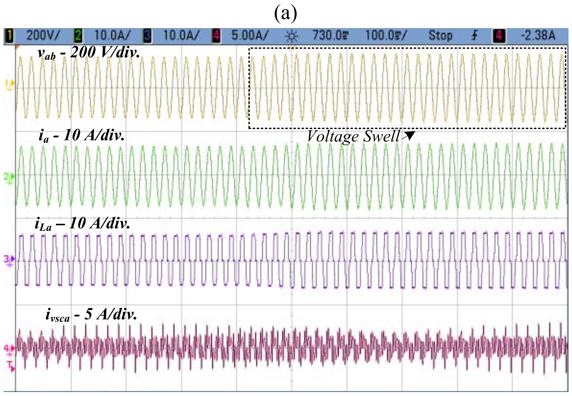

(b)

Fig. 9. Response of DSTATCOM system under voltage. (a) Sag. (b) Swell.

displacement factor (DPF), and values of THD in grid voltages and currents. The proposed system is performing under UPF mode. Fig. 4(c) shows magnitudes of the grid power, the load power and the VSC power. Here, the grid is supplying power to both load and VSC. Fig. 5(a) and (b) shows the harmonic spectrum and THD of grid current which is 2.92% and THD of the load current which is 25.58%. It is observed that THD in grid current is less than 5% which is acceptable to an IEEE-519 standard [20].

B. Responses Under Unbalanced Loads

Fig. 6(a)–(c) shows responses of proposed control algorithm and the system when subject to unbalanced nonlinear load. Fig. 6(a) depicts the response of the internal signals (G_{cp}, G_{Lp}, G_p, and i_b*) when phase "b" of nonlinear load is reconnected to the system. It is understood that on reconnecting the phase "b" load, weights in conductance and reference grid current are also increased. In Fig. 6(b) and (c), the waveforms of V_{dc}, i_b, i_c, i_{Lb}, i_{Lc}, i_{vscb}, i_{vscc}, and v_{bc} are shown when phase "b" load is reconnected. It is observed that on reconnecting the load, the grid currents are also increased and remain sinusoidal while dc bus voltage is maintained at set value. Moreover, it is observed that compensator supplies sinusoidal current in phase "b," while the load is disconnected.

It is also observed from Fig. 6(c) the variations in response of the signals of other phase "c" when the load is reconnected in phase "b."

TABLE II

COMPARISON OF PROPOSED NN-BASED ALGORITHM WITH CONVENTIONAL ALGORITHMS

Parameter	Proposed NN Based Algorithm	SRFT	LMS
Complexity	Low	High	Low
No. of Computation	Low	High	Low
DC link voltage Oscillation	Low	High	Medium
Accuracy	High	Medium	Poor
THDs in grid currents	Low	Medium	Medium
DSP Speed	High	Low	High
Sampling Time	30 μs	40 μs	30 μs

C. Performance Under Distorted Grid Voltages

Fig. 7(a)–(d) depicts response of system subjected to distortions in grid voltages. Fig. 7(a) and (b) shows amplitude of the parameters and waveforms of the system without DSTATCOM. It is seen that the THD of voltages is greater than 5%, while THD of grid currents is equal to load currents, i.e., 25%. Moreover, the DPF is decreased to 0.926. When DSTATCOM is switched "ON" as gating pulses are given to converter, it is seen from Fig. 7(c) and (d); grid voltages and currents are sinusoidal operating at UPF, and THDs in grid currents and voltages are reduced to less than 5%.

D. Performance Under Grid Voltages Imbalance

The responses of system under imbalance condition in grid voltages are shown in Fig. 8(a) and (b). Fig. 8(a) depicts magnitudes of the grid voltages, and it is observed that the imbalances in the voltages is approximately 25 V among "v_{ab}," "v_{bc}," and "v_{ca}." However, the grid currents are maintained sinusoidal and system performs satisfactory. Moreover, THDs in grid currents and voltages are less than 5% which are within limits of an IEEE-519 standard [20].

E. Performance Under Grid Voltages Sag/Swell

The performance of the system under grid voltage sag and swell condition is shown in Fig. 9(a) and (b), respectively, showing the waveforms of v_{ab}, i_a, i_{La}, and i_{vsca}. With the 12% sag in grid voltage as shown in Fig. 9(a), the grid current and the load current are decreased, while the DSTATCOM operates satisfactorily. Similarly, with 12% swell in grid voltage as shown in Fig. 9(b), the grid current and the load current are increased, while DSTATCOM operates satisfactorily.

F. Comparison of Proposed Admittance-Based NN Control Algorithm With Conventional Algorithms

Table II shows the comparison of proposed NN-based algorithm with conventional algorithms such as synchronous reference frame (SRF) theory and LMS. The proposed algorithm has low complexity, less number of computations, and high accuracy due to simple addition and multiplication blocks with respect to SRF-theory-based control algorithm which is based on d-q transformations and requires phase-locked loop block to extract the grid angle. Due to less number of computations, it has high DSP speed and less sampling time. Due to reduced mean-square error, it has an improved performance at steady-state and dynamic conditions, thereby low oscillation in dc-link voltage and low THD in grid current.

VI. Conclusion

An admittance LMS-based NN control algorithm for a DSTATCOM for enhancing the power quality of a three-phase distribution network subjected to nonlinear and unbalanced loading under distorted and imbalanced three-phase voltages at the PoI has been simulated and implemented in the laboratory. This admittance LMS-based NN structure has a simple architecture which reduces the computational complexity and burden, which makes it easy to implement. Test results have shown satisfactory operation of system at UPF under abnormal conditions of distribution network such as noise, distortion in voltage, imbalance in three-phase voltages, and unbalanced loads at PoI. Moreover, the THD in grid currents and grid voltages of the system have obeyed to an IEEE-519 standard.

Appendix

A. Simulation Model Parameters

DC bus voltage, $V_{\mathrm{dc}} = 700$ V; interfacing inductor, $L_f = 2.9$ mH; dc-link capacitor $C_{\mathrm{dc}} = 5000$ μF; sampling time, $T_s = 1$ μs; ripple filter, $R_f = 5$ Ω and $C_f = 10$ μF; grid voltage, $V_{\mathrm{ab}} = 415$ V (rms); and load = diode bridge with $R = 40$ Ω and $L = 150$ mH load. DC PI controller, $K_{\mathrm{pd}} = 0.5$ and $K_{\mathrm{id}} = 0.5$ and $\sigma_p = 0.95$.

B. Experimental System Parameters

$V_{\mathrm{dc}} = 380$ V; $C_{\mathrm{dc}} = 9400$ μF; $L_f = 2.9$ mH; $T_s = 30$ μs; $V_{\mathrm{ab}} = 210$ V (rms); $R_f = 5$ Ω and $C_f = 10$ μF; $K_{\mathrm{pd}} = 9.5$ and $K_{\mathrm{id}} = 0.1$; $\sigma_p = \sigma_q = 0.85$; and nonlinear load = diode bridge with 2.5-kW load.

Acknowledgment

The authors would like to thank the Department of Science and Technology, Government of India, for supporting project under Grant RP02583.

References

[1] S. Haykin, *Neural Networks and Learning Machines*, 3rd ed. Upper Saddle River, NJ, USA: Pearson Education, 2009.
[2] S. Xie, W. Zhong, K. Xie, R. Yu, and Y. Zhang, "Fair energy scheduling for vehicle-to-grid networks using adaptive dynamic programming," *IEEE Trans. Neural Netw. Learn. Syst.*, vol. 27, no. 8, pp. 1697–1707, Aug. 2016.
[3] S. Mishra, "Neural-network-based adaptive UPFC for improving transient stability performance of power system," *IEEE Trans. Neural Netw.*, vol. 17, no. 2, pp. 461–470, Mar. 2006.
[4] G. K. Venayagamoorthy, R. K. Sharma, P. K. Gautam, and A. Ahmadi, "Dynamic energy management system for a smart microgrid," *IEEE Trans. Neural Netw. Learn. Syst.*, vol. 27, no. 8, pp. 1643–1656, Aug. 2016.
[5] A. M. Munoz, *Power Quality Mitigation Technologies in a Distributed Environment*. London, U.K.: Springer, 2007.
[6] F. Shahnia, S. Rajakaruna, and A. Ghosh, *Static Compensators (STATCOMs) in Power Systems*. Singapore: Springer, 2015.
[7] B. Singh, A. Chandra, and K. Al-Haddad, *Power Quality: Problems and Mitigation Techniques*. Hoboken, NJ, USA: Wiley, 2015.
[8] M. V. M. Kumar, M. K. Mishra, and C. Kumar, "A grid-connected dual voltage source inverter with power quality improvement features," *IEEE Trans. Sustain. Energy*, vol. 6, no. 2, pp. 482–490, Apr. 2015.
[9] C. Kumar and M. K. Mishra, "Operation and control of an improved performance interactive DSTATCOM," *IEEE Trans. Ind. Electron.*, vol. 62, no. 10, pp. 6024–6034, Oct. 2015.
[10] M. Srinivas, I. Hussain, and B. Singh, "Combined LMS-LMF based control algorithm of DSTATCOM for power quality enhancement in distribution system," *IEEE Trans. Ind. Electron.*, vol. 63, no. 7, pp. 4160–4168, Jul. 2016.
[11] M. Badoni, A. Singh, and B. Singh, "Variable forgetting factor recursive least square control algorithm for DSTATCOM," *IEEE Trans. Power Del.*, vol. 30, no. 5, pp. 2353–2361, Oct. 2015.
[12] S. C. Hsieh, "Economic evaluation of the hybrid enhancing scheme with DSTATCOM and active power curtailment for PV penetration in Taipower distribution systems," *IEEE Trans. Ind. Appl.*, vol. 51, no. 3, pp. 1953–1961, May 2015.
[13] B. Singh, S. S. Murthy, R. R. Chilipi, S. Madishetti, and G. Bhuvaneswari, "Static synchronous compensator-variable frequency drive for voltage and frequency control of small-hydro driven self-excited induction generators system," *IET Generat., Transmiss. Distrib.*, vol. 8, no. 9, pp. 1528–1538, Sep. 2014.
[14] A. Tilli and C. Conficoni, "Control of shunt active filters with actuation and current limits," *IEEE Trans. Control Syst. Technol.*, vol. 24, no. 2, pp. 644–653, Mar. 2016.
[15] B. Widrow, M. J. McCool, M. Larimore, and C. R. Johnson, "Stationary and non-stationary learning characteristics of the LMS adaptive filter," *Proc. IEEE*, vol. 64, no. 8, pp. 1151–1162, Aug. 1976.
[16] G. Carvajal, M. Figueroa, D. Sbarbaro, and W. Valenzuela, "Analysis and compensation of the effects of analog VLSI arithmetic on the LMS algorithm," *IEEE Trans. Neural Netw.*, vol. 22, no. 7, pp. 1046–1060, Jul. 2011.
[17] B. Chen, Y. Zhu, and J. Hu, "Mean-square convergence analysis of ADALINE training with minimum error entropy criterion," *IEEE Trans. Neural Netw.*, vol. 21, no. 7, pp. 1168–1179, Jul. 2010.
[18] Z.-Q. Wang, M. T. Manry, and J. L. Schiano, "LMS learning algorithms: Misconceptions and new results on converence," *IEEE Trans. Neural Netw.*, vol. 11, no. 1, pp. 47–56, Jan. 2000.
[19] P. E. An, M. Brown, and C. J. Harris, "On the convergence rate performance of the normalized least-mean-square adaptation," *IEEE Trans. Neural Netw.*, vol. 8, no. 5, pp. 1211–1214, Sep. 1997.
[20] *IEEE Recommended Practices and requirement for Harmonic Control on Electric Power System*, IEEE Standard 519, 1992.
[21] *IEEE Recommended Practice for the Analysis of Fluctuating Installations on Power Systems*, IEEE Standard 1453-2015, 2011.
[22] H. Akagi, E. H. Watanabe, and M. Aredes, *Instantaneous Power Theory and Applications to Power Conditioning*. New York, NY, USA: Wiley-IEEE Press, Jul. 2009.
[23] N. Mohan, T. M. Undeland, and W. P. Robbins, *Power Electronics: Converters, Applications, and Design*. New Delhi, India: Wiley, 2003.

Rahul Kumar Agarwal was born in Adityapur, India, in 1990. He received the B.Tech. degree in electrical engineering from the Biju Patnaik University of Technology, Bhubaneswar, India, in 2012, and the M.Tech. degree in construction technology and management from the Department of Civil Engineering, IIT Delhi, New Delhi, India, in 2016.

In 2012, he joined Blue-Chip Company, Odisha, L&T Construction in Metallurgical and Material Handling Independent Company, as a Graduate Engineer Trainee. In 2013, he became a Senior Electrical Engineer, where he was in-charge of the Plant and Machinery Department, L&T-Coal Handling Plant, Lalitpur, India. His current research interests include power quality, distribution static compensator, and solar energy systems.

Ikhlaq Hussain (M'14) was born in Doda, India, in 1986. He received the B.E. degree in electrical engineering from the University of Jammu, Jammu, India, in 2009, and the M.Tech. (Gold Medalist) degree in electrical power system management from Jamia Millia Islamia (A Central University), New Delhi, India, in 2012. He is currently pursuing the Ph.D. degree with the Department of Electrical Engineering, IIT Delhi, New Delhi.

In 2012, he was a Lecturer with the Department of Electrical Engineering, National Institute of Technology, Srinagar, India. His current research interests include power electronics, power quality, custom power devices, renewable energy systems, power system management, and microgrid.

Mr. Hussain was a recipient of the POSOCO Power System Award from Power System Operation Corporation Limited, India, and the Foundation for Innovation and Technology Transfer at IIT Delhi in 2017, the IEEE INDICON Best Paper Award in 2015, and the IEEE UPCON Best Paper Award in 2016.

Bhim Singh (SM'99–F'10) was born in Rahamapur, Bijnor India, in 1956. He received the B.E. degree in electrical engineering from the University of Roorkee, Roorkee, India, in 1977, and the M.Tech. degree in power apparatus and systems and the Ph.D. degree from IIT Delhi, New Delhi, India, in 1979 and 1983, respectively.

In 1983, he joined the Department of Electrical Engineering, University of Roorkee (now IIT Roorkee), as a Lecturer. He became a Reader in 1988. In 1990, he joined the Department of Electrical Engineering, IIT Delhi, as an Assistant Professor, where he became an Associate Professor in 1994 and a Professor in 1997. From 2014 to 2016, he was the Head of the Department of Electrical Engineering at IIT Delhi, where he is currently the Dean Academics with IIT Delhi. His current research interests include Photovoltaic (PV) grid interface systems, microgrid, power quality, PV water pumping systems, power electronics, electrical machines, drives, FACTS, and HVDC systems.

Prof. Singh is a Life Member of the Indian Society for Technical Education and the System Society of India. He is a fellow of the Indian National Academy of Engineering, the National Academy of Sciences, India, the Indian Academy of Sciences, the Institution of Engineering and Technology, U.K., the Institution of Engineers (India), and the Institution of Electronics and Telecommunication Engineers. He has guided 65 Ph.D. dissertations and 162 M.E./M.Tech./M.S.(R) theses. He has executed more than 75 sponsored and consultancy projects.